INS-NUMA-19

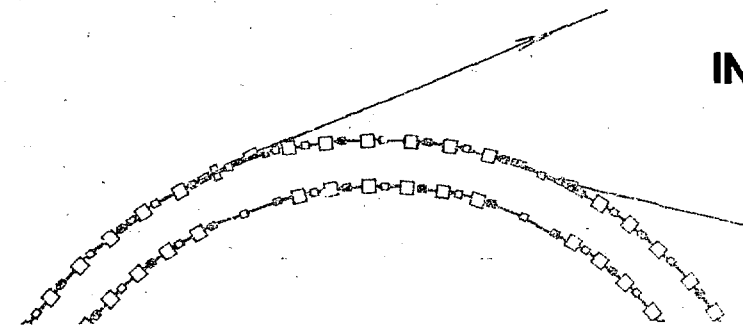

Multiwire and Single Rod Beam Profile Monitors in the TARN

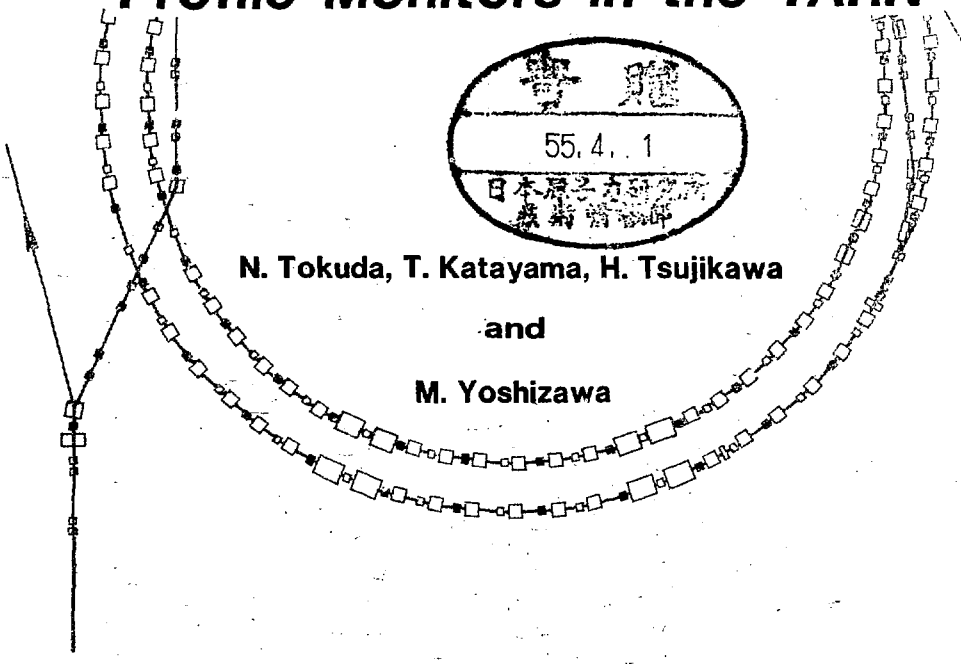

N. Tokuda, T. Katayama, H. Tsujikawa

and

M. Yoshizawa

March, 1980

STUDY GROUP OF NUMATRON AND
HIGH-ENERGY HEAVY-ION PHYSICS
INSTITUTE FOR NUCLEAR STUDY
UNIVERSITY OF TOKYO
Midori-Cho 3-2-1, Tanashi-Shi,
Tokyo 188, Japan

Multiwire and Single Rod Beam Profile Monitors in the TARN

N. Tokuda, T. Katayama, H. Tsujikawa and M. Yoshizawa

Institute for Nuclear Study, University of Tokyo

Tokyo, Japan

Abstract

Beam profile monitors have been constructed to examine characteristics of the TARN; the profile and the orbit of an injected beam and the displacement of the beam orbit due to the sweep of RF frequency. We prepared two kinds of sensers, i.e. a multiwire chamber and a single rod, in which the beam is stopped. A beam stopper is also prepared to measure the intensity of the injected beam. Each senser is attached to a driving apparatus with a pulse motor operated remotely in the control room. A read-out circuit is prepared for the multiwire monitor. As well as the construction of the monitor system, the characteristics of the TARN obtained by the monitors are briefly described.

Introduction

Destructive type beam monitors are installed in the TARN. Though they cannot be used in the process of beam stacking, they have better detection sensitivity, and provide the more detailed position and the profile of the beam than a non-destructive type beam monitor. They are used for the ajdustment of the injection and the magnet systems in an injection stage and for the measurement of the relation between a beam orbit and an RF frequency.

Three kinds of sensers are prepared: One is a rod of Be-Cu (Beryllium-Copper), another is comprized of sixteen Be-Cu ribbons, and the other is a plate of tantalum. In the first and the last the rod or the plate is connected to a nano-ammeter, and in the second the charges in each of the ribbons are transferred to a condenser in a read-out circuit and the voltage across the condenser is measured at every injection of 40 Hz. Each senser is attached to a driving apparatus with a pulse motor operated in the control room of the TARN. The position of a senser is monitored using a potentiometer.

The sensers are thick enough to stop the beam in them in order to measure an accurate beam current and to obtain a sufficient large signal level. The characteristics of the TARN have been investigated with H_2^+ and He^{2+} beams of 7 MeV/u, because the dissociation cross section of H_2^+ is as large as the charge exchange cross sections of heavy ions with residual gas molecules, and a long life time is available with He^{2+} beam. The range in copper of these beams is 117 mg/cm^2,

or 0.13 mm in thickness, and 186 mg/cm^2 or 0.112 mm in tantalum. It is goaled at the TARN to accumulate $^{14}N^{5+}$ ions of 7 MeV/u, of which the range in copper is 75 mg/cm^2 or 0.083 mm thick, and 125 mg/cm^2 and 0.075 mm in tantalum. Therefore a Be-Cu rod of 3 mm in diameter, 0.5 mm thick Be-Cu ribbons, and a 0.3 mm thick tantalum plate are prepared.

The multiwire beam profile monitor is used in the stage of beam injection into the TARN. The final parts of the beam transport system, the injection and the magnet system are adjusted according to the measured profile and the position. A couple of monitors are installed at a setting position to measure the beam profile in horizontal and vertical directions. The rod monitor moving horizontally is used for the measurement of displacement of the beam orbit with the sweep of RF frequency, as well as the beam profile. The tantalum plate drops to the orbit plane and measures the intensity of the injected beam.

The arrangement of these monitors in the TARN is shown in Fig. 1.

Chamber of the Multiwire Monitor

The chamber consists of sixteen Be-Cu ribbons fixed within a positioning accuracy of ±0.2 mm on a ceramic frame 3 mm in thickness as in Fig. 2. The sizes of one ribbon are 2 mm in width, 0.5 mm in thickness and 70 mm in length, and the gap between adjacent ribbons is 1 mm. As the chamber is mounted in a vacuum chamber of lower than 10^{-10} Torr, and must be bakable at 250°C, solder is not used for the fixation of the ribbons and lead wires on the ceramic frame. The ribbons

and lead wires are joined respectively with spot-welding and silver solder to pins sticked in the ceramic frame. The lead wires linking the chamber and feedthrough are copper of 0.6 mm in diameter coated with polyimid of which the electrical insulation is guaranteed up to 250°C. The feedthrough with 22 pins is ultra-high vacuum tight with ceramic insulator and is bakable.

No cooling device is equipped to the chamber against the heating by the beam, because the temperature at the chamber is estimated to be kept lower than 100°C. The estimation is on the assumption that heat inflow due to beam's energy loss in the ribbon equals to outflow due to radiation to vacuum and conduction through the lead wire. The inflow is calculated to 4×10^5 erg/s for a 7 MeV/u $^{14}N^{5+}$ beam, where the beam pulse is assumed to 2 μA at peak intensity and 20 μs in width, and the repetition rate 50 Hz. At the equilibrium temperature of 74°C, outflow balances with the inflow; 3×10^5 erg/s due to radiation and 1×10^5 erg/s due to conduction.

Driving Apparatus

The driving apparatus is designed considering it is installed in an ultra-high vacuum system and the senser must be positioned with accuracy. From the vacuous point of view the apparatus is made only of metal but not of organic material with high outgassing rate. Parts are welded at the vacuum side as far as possible not to make a harmful chink for the ultra-high vacuum. The structure is fit for evacuation and

proof against the repetition of baking performed at 250°C ∿ 300°C for two days a month. The apparatus is worked by a pulse motor at remote operation, or by hand at the calibration of a potentiometer for the remote measurement of the senser's position. Twelve apparatusus are prepared: The four are of a 210 mm stroke, and the eight of 60 mm.

Figure 3 shows the structure of the assembly. In a driving mechanism a cylinder with square threads on its in- and outsides is used (a in Fig. 3). It realizes a compact and light assembly of a hang-over style and an accurate positioning of the senser, because its backlash is smaller than that of an ordinary gear system. The shaft with a senser (b) is moved by the rotation of the threaded cylinder. The position of the senser is indicated by a rod (c) fixed to a ring geared with the cylinder. Only welded bellows (d) are used as moving parts in the vacuum environment. The shaft bearing (e) is made of beryllium-copper with small sliding friction. In the apparatus of a 210 mm stroke another bearing is used against the deflection of the bellows. The bearing are holed for efficient evacuation. Through the shaft of a pipe the lead wires from the senser are connected to a feed-through (f).

The accuracy of senser's positioning is examined, and it turns out that the fluctuation of the moved distances is within ±0.1 mm, when pulses of the number corresponding to the full stroke of 60 mm or 210 mm are supplied.

Figure 4 shows the driving apparatus attached to a vaccum chamber in the ring.

Operation system

Twelve monitors are installed in the TARN and at the end parts of the beam transport line. Each of the driving apparatuses with a pulse motor is operated by a pulse generating circuit in the control room. The schematic diagram of the operation system is shown in Fig. 5.

In the control room the selection of a driving apparatus and feeding of pulses for the driving of a pulse motor are performed, and the position of the senser is monitored. The twelve driving apparatuses are divided into three groups, each of which is provided with a driver circuit for the supply of pulsed current, produced by chopping a DC voltage from a DC power supply, to a pulse motor. Three sets of the driver circuit, the DC power supply and a relay box is placed near the monitors.

Read-out circuit

The charges of the beam stopped in the multiwire chamber are read out through a circuit.[1,2] The diagram and the time chart are shown in Figs. 6 and 7, respectively. The circuit is made on a printed circuit board, and set in a two span NIM module.

Each of the chamber is connected to a 1000 pF precision mylar condenser through a resistor of 100 Ω to integrate the charge in the ribbon. For a protection of the electronics, low leakage diodes (1S1553) are used as a limiting circuit to prevent the capacitor voltage

from exceeding safe values in the event that the capacitors are not discharged periodically and the charge are accumulated in the condenser. The diode is of a precision type, still it has a deviation in reverse current which brings about the unflatness of the ground level. Also the deviation of capacitances of integrating condensers results in the unflatness. Careful selection of the diodes improves remarkably the unflatness as is shown in Figs. 8(a) and (b).

The interconnection of the each ribbon and the capacitor is converted to the inputs of a complementary MOS FET multiplexer (DG 506) through a high resisteance of 1 MΩ. The multiplexer has a high "OFF" resistance ($\sim 10^8$ Ω) and a low "ON" one (~ 500 Ω). The output of the multiplexer is connected to the gate of an FET output amplifier and to the drain of the PET for discharging. The input impedance of the output amplifier is high enough ($\sim 10^8$ Ω) compared to the "ON" resistance of the multiplexer. As a result the droop in capacitor voltage is negligible during the sampling time of 0.5 ms. The multiplexer with a single-pole 16 position electronic switch is controlled by a 4 bit binary word inputs and an enable-inhibit input. The synchronous up/down counter (74193) regulates the sequential selection of the "ON" position of the multiplexer. The sampling rate can be varied by an oscillator (NE 555V) and is usually 2.0 kHz. After the beam gate signal is finished, the start pulse can initiate the sampling by the clock pulse.

The circuit is positioned near the beam monitor, and its signal input is connected to the feed through at the driving apparatus by a 2 m long multicored cable.

Results

Figures 9 (a) and (b) show the profile of 14 MeV H_2^+ beam at p17 in the transport line. The widths of the beam are $\sim$12 mm in horizontal and $\sim$9 mm in vertical. The expected full widths of the beam are given by

$$w_x = 2\sqrt{\beta_x \varepsilon_x} + \eta \frac{\Delta p}{p} \quad ,$$

$$w_y = 2\sqrt{\beta_y \varepsilon_y} \quad ,$$

where β is the beta functions, ε the emittances, η the dispersion function, $\Delta p/p$ the momentum spread. These values at p17 are numerically

$$\beta_x = 7.95 \text{ m.}$$

$$\beta_y = 6.48 \text{ m.}$$

$$\varepsilon_x = 2.20 \text{ mm}\cdot\text{mrad},$$

$$\varepsilon_y = 6.18 \text{ mm}\cdot\text{mrad},$$

$$\eta = 0.109 \text{ m},$$

$$\Delta p/p = 1/1600,$$

where β- and η- functions are from the program "MAGIC", and ε and $\Delta p/p$ are measured. Substituting these values to the above equations,

$$w_x = 8.43 \text{ mm} ,$$

$$w_y = 12.65 \text{ mm} .$$

A bending magnet and quadrupole magnets are adjusted to an optimum condition according to these beam profiles.

Figure 10 shows the horizontal profile of the injected beam detected by the multiwire monitor. The observation of the position and the profile is successively performed at points from S2 to S8, and the bending and quadrupole magnets as well as the inflector are adjusted.

Figure 11 shows the two orbits of the injected beam without multiturn. The monitor is at S8. The right peak is due to the beam in the first turn and the left in the second and the fourth turns. As the ν-value in the horizontal direction is designed to 2.25 and the injection position is 30 mm from the central orbit, the position of the injected beam in the first turn is expected to be at 30 mm and that in the second and the fourth to be on the central orbit. The measured value agrees with the expected one. The peak due to the beam in the third turn, which is not observed in the picture, is confirmed by displacing the chamber.

Figure 12 shows the distribution of the beam injected by the multiturn method, which is observed by the rod monitor. The width of the whole beam injected successively is 35 mm. The emittance is given by

$$x_\beta = \sqrt{\beta \varepsilon} ,$$

where x_β is the half width of the beam and is 35/2 mm, β_x the beta function and 2 m according to the program "SYNCH", ε the emittance. It is calculated the 153 mm·mrad, while the designed value is 102.9 mm·mrad.[3)]

The displacement of the beam orbit with the sweep of RF frequency is measured by this monitor, and the result is shown in Fig. 13. The beam is 7 MeV/u He^{2+}. The measured value of df/dx at the injection orbit, or at $\Delta x = 0$, is 3.7 kHz/mm, where calculated value is 4.45 kHz/mm. They agree fairly well with each other. This factor is calculated by

$$\frac{df}{dx} = \left(\frac{1}{\gamma^2} - \frac{1}{\gamma_t^2}\right) \frac{f}{\eta} \quad ,$$

where f is the RF frequency, x the position, γ the Lorentz factor, γ_t the transition parameter, η the dispersion function. These parameters are numerically

$$f = 8.027 \text{ MHz} \ ,$$

$$\gamma = 1.00752 \ ,$$

$$\gamma_t = 1.980 \ ,$$

$$\eta = 1.316 \text{ m} \ ,$$

where values of γ_t and η are according to SYNCH, and

$$\frac{df}{dx} = 4.45 \text{ kHz/mm} \ .$$

Conclusion

We have constructed three kinds of destructive beam position-and-profile monitors, which are useful for the determination of beam characteristics such as the position of injection orbit and the shift of the equilibrium orbit by the sweep of RF frequency as well as the beam profile. The senser of the monitor was moved by the pulse motor and it could be set with a precision of ±0.1 mm. The results of the measurement show that the beam profile at the 7th straight section is 35 mm, when the multiturn inejction is performed and the shift of the orbit by the RF field is 0.27 mm/kHz, where the calculated one by the "SYNCH" program is 0.22 mm/kHz. By use of the digital control system for the driving mechanism, the computer ocntrol and data-logging are available and will be performed in near future.

Acknowledgment

The authors would like to express their thanks to Mr. S. Watanabe for his very useful discussions about the electronic system, to Prof. Y. Hirao for his continuous encouragement through the work, and to Irie Koken Co. Ltd. for the skillful manufacturing of driving apparatuses.

References

1. F. Hornstra, Jr. and J. R. Simanton, Nucl. Instr. and Meth., 68 (1969) 138.

2. S. Arai, K. Gomi, H. Okuno and K. Katsuura, INS, University of Tokyo, report INS-TH-103, 1975, (in Japanese).

3. S. Yamada and T. Katayama, INS, University of Tokyo, report, INS-NUMA-12, 1979.

Figure Captions

Fig. 1 Arrangement of the beam profile monitors and the stopper in the TARN and the transport line. The single rod monitor and the stopper are set at S7, and the multiwire ones are at the other places, shadowed in black.

Fig. 2 Chamber of the multiwire monitor.

Fig. 3 Drawing of the driving apparatus of a 210 mm stroke. a; threaded cylinder, b; senser, c; position indicator, d; welded bellows, e, e'; bearings, f; feedthrough, g; pulse motor, h; potentiometer, i; limit switch.

Fig. 4 Driving apparatus attached to the vacuum chamber in the ring. A couple of the multiwire monitors are seen.

Fig. 5 Block diagram of the control system for pulse motors.

Fig. 6 Diagram of the read-out circuit for the multiwire monitor.

Fig. 7 Time chart of the read-out circuit.

Fig. 8 The unflatness of the output ground level was improved by selection of diodes. (a); before the improvement. (b); improved.

Fig. 9 Horizontal (a) and vertical (b) beam profiles at p16 in the transport line.

Fig. 10 Horizontal beam profile of an injected beam detected by the multiwire monitor at S8.

Fig. 11 Two of the three peaks of the injected beam observed by the multiwire monitor at S8.

Fig. 12 Profile of the beam injected by multiturn detected by the single rod monitor.

Fig. 13 Displacement of the beam orbit due to the sweep of RF frequency. At the injection orbit $\Delta x = 0$ mm, and the RF frequency is 8.027 MHz. The data are fitted by a straight line with a coefficient of 3.7 kHz/mm.

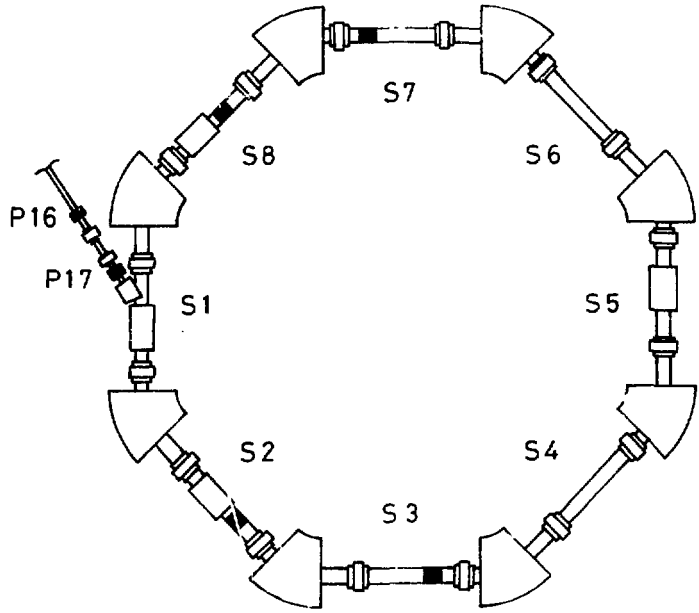
S7
S8
S6
P16
P17
S1
S5
S2
S4
S3

Fig. 1

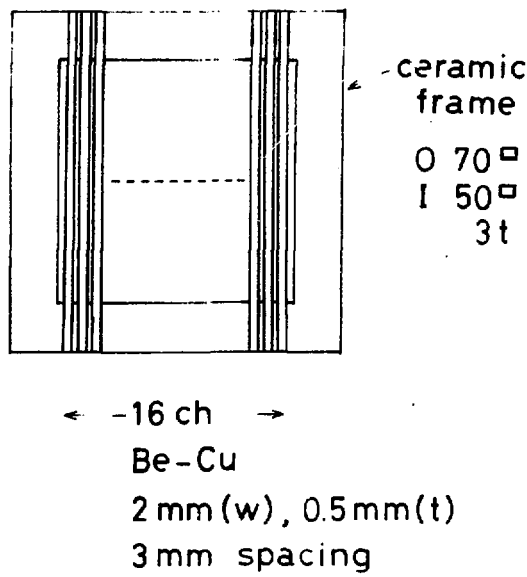
ceramic
frame
O 70□
I 50□
3t
-16 ch
Be-Cu
2 mm (w), 0.5 mm (t)
3 mm spacing

Fig. 2

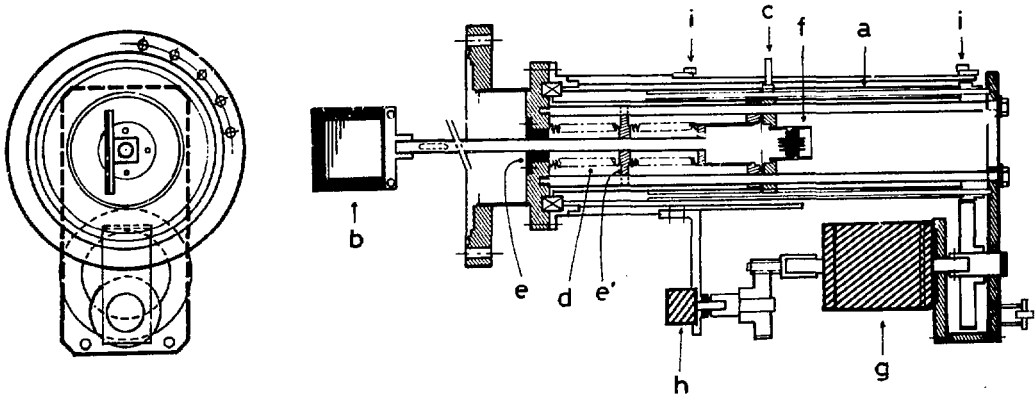

Fig. 3

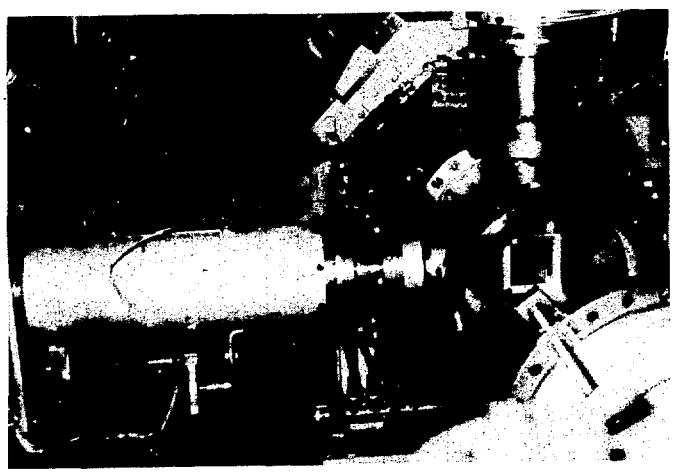

Fig. 4

Diagram of the Control of Pulse Motors

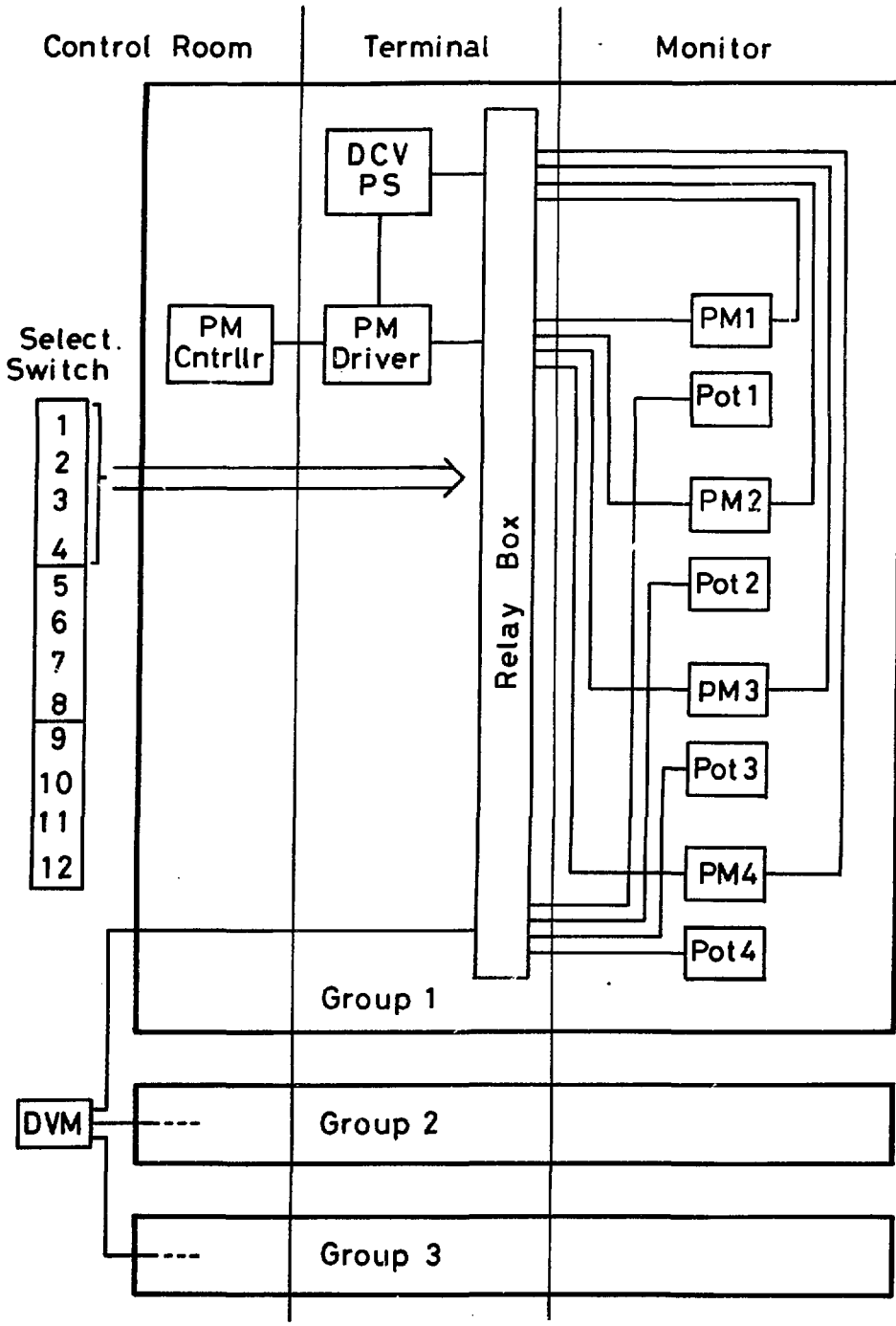

Fig. 5

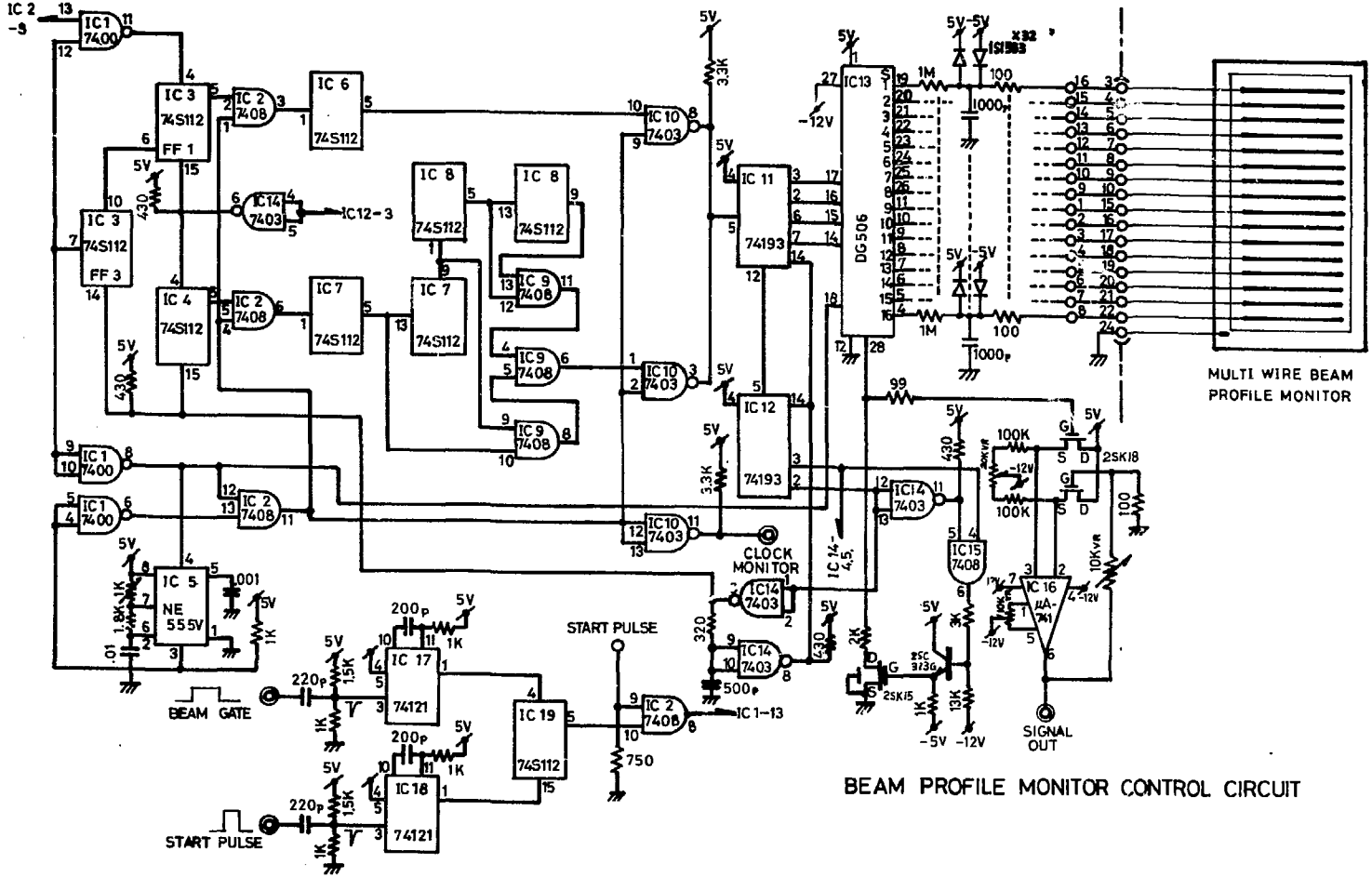
MULTI WIRE BEAM PROFILE MONITOR
BEAM PROFILE MONITOR CONTROL CIRCUIT
BEAM GATE
START PULSE
CLOCK MONITOR
SIGNAL OUT
IC 1-13
IC12-3
IC 14-4,5,
IC 1 7400
IC 2 7408
IC 3 74S112 FF 1
IC 3 74S112 FF 3
IC 4 74S112
IC 5 NE 555V
IC 6 74S112
IC 7 74S112
IC 8 74S112
IC 9 7408
IC 10 7403
IC 11 74193
IC 12 74193
IC13 DG506
IC14 7403
IC15 7408
IC 16 μA-741
IC 17 74121
IC 18 74121
IC 19 74S112
2SK18
2SK15
2SC 373G
5V
-5V
-12V

Fig. 6

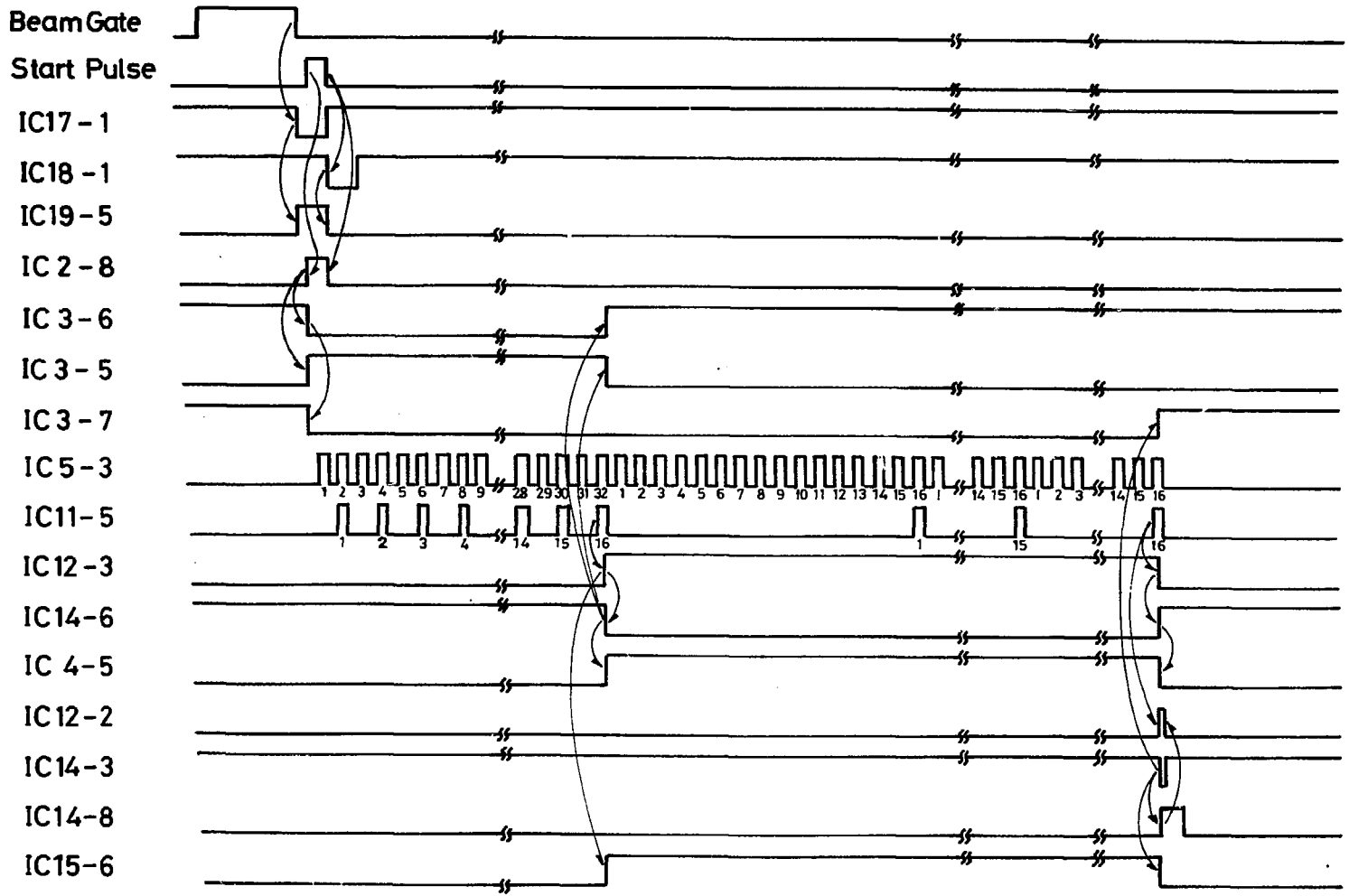
Beam Gate
Start Pulse
IC17 - 1
IC18 - 1
IC19 - 5
IC 2 - 8
IC 3 - 6
IC 3 - 5
IC 3 - 7
IC 5 - 3
IC11 - 5
IC12 - 3
IC14 - 6
IC 4 - 5
IC12 - 2
IC14 - 3
IC14 - 8
IC15 - 6

Fig. 7

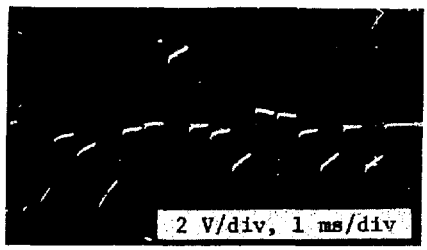

Fig. 8(a)

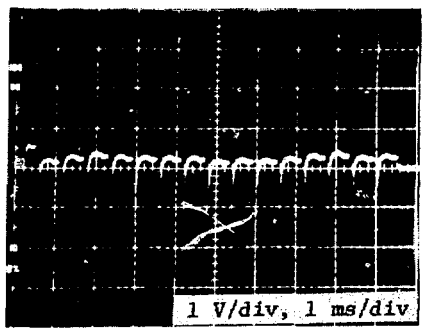

Fig. 8(b)

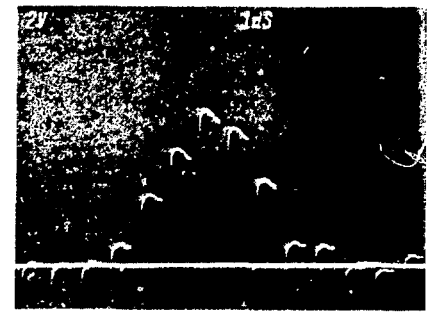

Fig. 9(a)

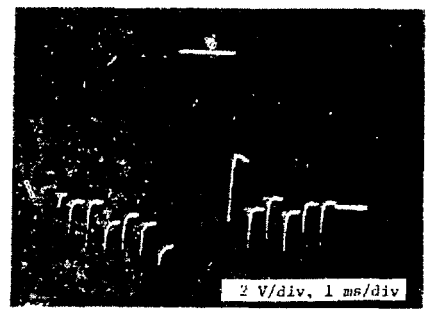

Fig. 9(b)

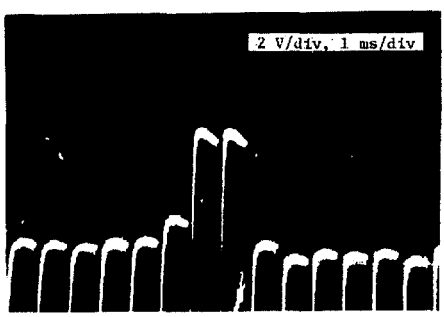

Fig. 10

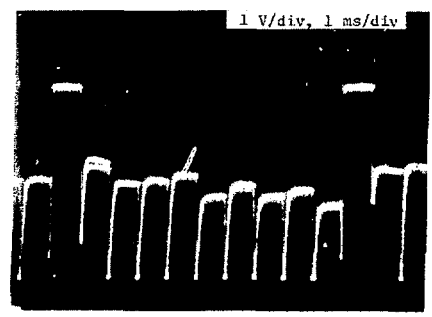

Fig. 11

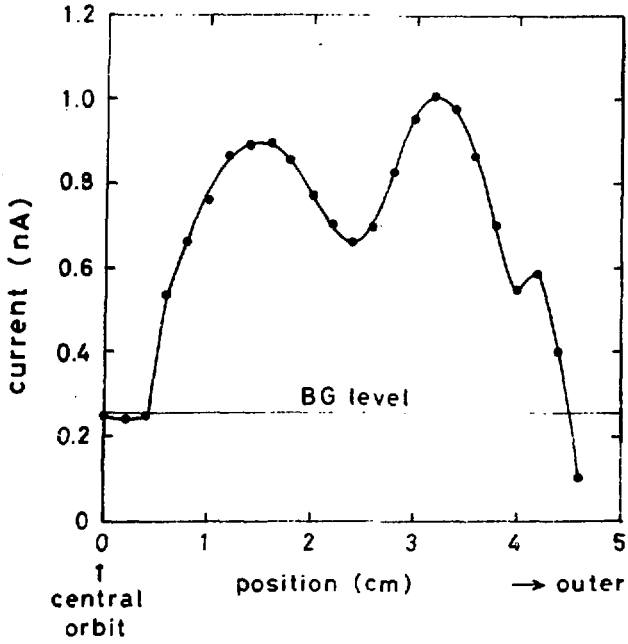
1.2
1.0
0.8
0.6
0.4
0.2
0
current (nA)
BG level
0
1
2
3
4
5
position (cm)
central orbit
outer

Fig. 12

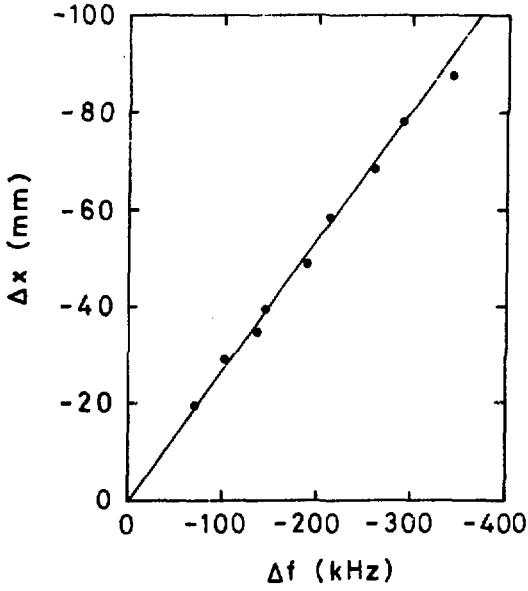
-100
-80
-60
-40
-20
0
Δx (mm)
0
-100
-200
-300
-400
Δf (kHz)

Fig. 13